Self-assembly of an Organometallic Fe_9O_6 Cluster from Aerobic Oxidation of (tmeda)Fe($CH_2{}^tBu$)$_2$

Jonathan A. Kephart,[a]‡ Zachary Hecht,[a]‡ Brooke N. Livesay,[b] Dr. Matthew P. Shores,[b] Dr. V. Codrina Popescu,[c] Dr. Navamoney Arulsamy,[a] Dr. Elliott B. Hulley.*[a]

[a] Department of Chemistry, University of Wyoming
Laramie, WY 82071, USA

[b] Department of Chemistry, Colorado State University
Fort Collins, CO 80523, USA

[c] Department of Chemistry, University of St. Thomas
St. Paul, MN 55105, USA

Abstract: Substoichiometric aerobic oxidation of the high-spin organometallic compound (tmeda)Fe($CH_2{}^tBu$)$_2$ (tmeda = N,N,N',N'-tetramethylethylenediamine) in toluene or THF solution leads to the self-assembly of a magic-sized all-ferrous oxide cluster containing the **Fe_9O_6** subunit and bearing organometallic and diamine ligands. Mössbauer studies of the cluster and the reference complex (tmeda)Fe($OCPh_3$)$_2$ are consistent with the all-ferrous assignment, and magnetometry reveal considerable antiferromagnetic coupling between Fe atoms in the cluster and frustrated antiferromagnetic interactions between clusters in the solid state.

Molecular clusters are profoundly important species, playing fundamental roles in materials science, nanocatalysis and as models of heterogeneous surfaces and protein active sites.[1] Since aggregation steps are generally unselective and fast, synthetic routes towards large atomic assemblies that result in monodisperse samples are rare. Originally limited to time-controlled hydrothermal methods, recent developments have enabled the syntheses of atomically-precise ligand-stabilized clusters of transition metals and semiconductors,[2,3,12,4–11] wherein conditions are controlled to selectively aggregate monomers and minimize bulk material growth. As a result of these studies of mesoscale entities, the change in physical properties of materials as they progress from the molecular scale to the bulk can be studied in great detail. Since the development of nanoengineered materials (e.g. metal-organic frameworks) depends heavily on the available design elements,[13] modular clusters with a variety of chemical and physical properties are highly desirable.

Metal oxide clusters are of particular interest due to the electrical and magnetic properties of the bulk compounds. Transition metal oxide clusters have nearly always been studied as gas-phase species generated by laser ablation of metals in an oxygen atmosphere.[14–17] Synthetic routes towards chemically isolable atomically-precise clusters of these highly ionic materials are strongly hampered by the tendency for oxides to aggregate in the absence of polydentate ligand frameworks,[18,19] and syntheses are largely limited to hydrothermal conditions that result in carboxylate- or alkoxide-capped clusters and have limited opportunities for further elaboration into nanomaterials.[20–23] Moreover, since syntheses of hybrid MOF-like materials are often also hydrothermal,[13] the incorporation of oxide-based clusters can be complicated by annealing (changing the structure of the oxide subunit) or agglomeration. The present work reports the synthesis and unique magnetic properties of an atomically-precise ferrous oxide cluster of that bears highly reactive organometallic ligands, and represents the first synthetic route towards a member of the 'magic-sized' class of metal oxide clusters.[15,16]

While researching unrelated chemistry of first-row transition metal dialkyl compounds, we observed that exposure of organoiron compounds to sub-stoichiometric oxygen led to the formation of a hydrocarbon-soluble complex that crystallized on standing (Figure 1). Treatment of colorless (tmeda)Fe($CH_2{}^tBu)_2$ with 0.5 molar equiv. O_2 (from air) in toluene solution results in the formation of a red-brown solution/suspension. After stirring at room temperature for 4 hours and removal of solvent *in vacuo*, the brown/black residue was extracted with hydrocarbon solvents (e.g. pentane, hexane, heptane, etc.) to yield a brown solution from which deep red crystals of the nine-iron cluster **[Fe_9O_6]**•*solvent* formed (17 % isolated yield based on [Fe]).

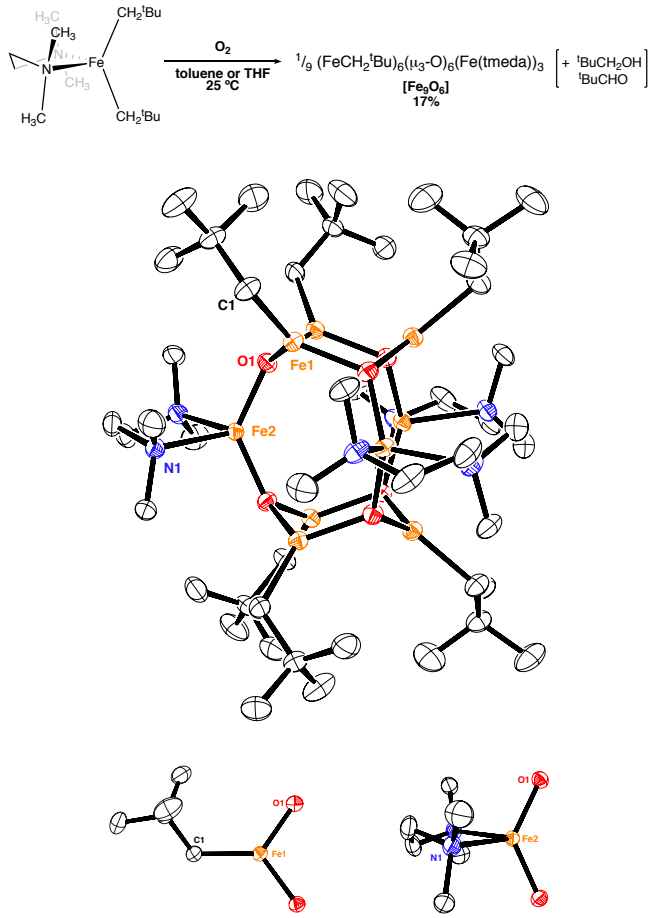

Figure 1. Synthesis (top), solid state structure of **[Fe_9O_6]** (middle) and views of the trigonal [(Np)FeO_2] (bottom right) and pseudotetrahedral [(tmeda)FeO_2] (bottom right) subunits. For clarity, the hydrogens are omitted and only the atoms of the first coordination sphere of the asymmetric unit are labelled. Selected distances and angles: d(Fe1-O1) = 1.907(2) Å, d(Fe1-O1') = 1.903(2) Å, d(Fe1-C1) = 2.060(3) Å, d(Fe2-O1) = 1.872(2) Å, d(Fe2-N1) = 2.232(2) Å, d(Fe1-Fe1') = 3.052(1) Å, d(Fe1-Fe2) = 3.249(1) Å, ∠(O1-Fe1-O1') = 110.08(9)°, ∠(O1-Fe2-O1') = 130.38(9)°.

Although the yield is relatively low, it is consistent for scales up to ~ 1g of (tmeda)Fe($CH_2{}^tBu)_2$ and is reasonable for a one-pot reaction that doesn't require ligands of additional complexity. The product is readily separated from the mother liquor by decantation; crystals of **[Fe_9O_6]** are attracted to an external permanent magnet with sufficient strength that this can be used to aid physical separation. Analysis of the mother liquor reveals the presence of neopentanol, pivalaldehyde, and residual

(tmeda)Fe($CH_2{}^tBu$)$_2$ which can be re-isolated *via* crystallization (~ 10 – 15% of the starting [Fe]). The relative amounts of oxidized organic products vary considerably from batch to batch.

The cluster crystallizes in the chiral rhombohedral space group $R3_2$, resulting in crystallographic D_3 symmetry, and possesses two distinct iron sites in either an axial or equatorial disposition (Figure 1, bottom). The coordination environment of the axial iron sites is best described as trigonal planar (Σ(angles) = 359.93º), whereas the equatorial iron sites are best described as distorted tetrahedral (τ_4 = 0.81).[24] The cluster is highly air- and moisture-sensitive, but is stable for days under ambient conditions in solution (toluene, benzene, THF) and indefinitely stable in the solid state. The cluster crystallizes on both the three-fold and perpendicular two-fold rotation axes of the crystal lattice, such that one sixth of the molecule is the asymmetric unit, and clusters pack such that they are mutually aligned on the *z*-axis (Figure 2).

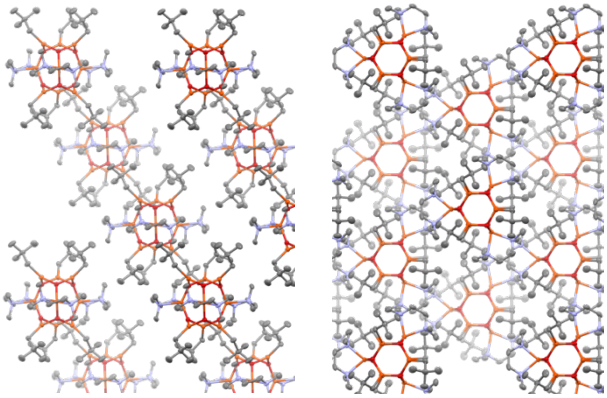

Figure 2. Depictions of the solid-state packing of **[Fe_9O_6]**. Views along the *a*-axis (left) and the *c*-axis (right) highlight the axial alignment and three-fold symmetric packing of **[Fe_9O_6]** molecules.

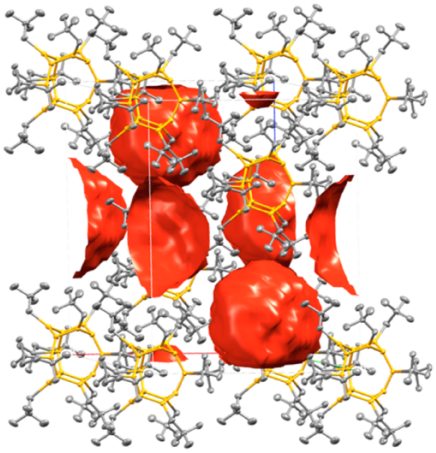

Figure 3. Depiction\ of the solid-state packing of **[Fe_9O_6]** highlighting the voids in the crystal lattice occupied by disordered solvent in **[Fe_9O_6]•**(pentane). For clarity, the Fe_9O_6 core is shown in yellow and the remaining ligands are shown in grey.

There are large voids between molecules (~ 50 Å^3) that contain disordered solvent molecules (Figure 3); isostructural crystals have been grown that contain C_nH_{2n+2} hydrocarbons (n = 5 – 9) and toluene, suggesting that crystal growth is somewhat

insensitive to the nature of the guest. This feature is very compelling for the design of complex materials, particularly given recent reports that exploit solid-state void space for the incorporation of electro- and/or magnetoactive guests.[9]

Redox-active metal centers in cluster compounds, particularly those with covalent bridging ligands (i.e. 'soft' anions), are notoriously challenging to assign to oxidation states.[25,26] In the present case, standard charges on ligands would predict that the average oxidation state of the nine iron atoms would be +2 (i.e. all ferrous). Zero-field Mössbauer spectroscopy at 5.5 K reveals two quadrupole doublets in a 2:1 ratio (labeled δ_1 and δ_2, respectively), as expected for the two distinct iron environments of **[Fe$_9$O$_6$]** (Figure 4, top). The major doublet (δ_1 = 0.41(2) mm/s, ΔE_Q = 1.57(2) mm/s), consistent with the trigonal planar environment on the axial sites, has spectral parameters similar to the high-spin trigonal-planar ferrous complex (nacnac)FeMe reported by Holland and coworkers (δ = 0.48 mm/s, ΔE_Q = 1.74 mm/s).[27] The minor doublet (δ_2 = 0.92(4) mm/s, ΔE_Q = 1.18(4) mm/s) should thus correspond to the pseudotetrahedral environment on the equatorial sites, although the relative paucity of Mössbauer spectra available for such an environment required the synthesis of a model complex. Treatment of (tmeda)Fe($CH_2{}^tBu$)$_2$ with two equivalents of triphenylmethanol yields the high-spin ferrous alkoxide (tmeda)Fe($OCPh_3$)$_2$, which exhibits a Mössbauer spectrum (Figure 4, bottom) that is indeed consistent with the minor component in the spectrum of **[Fe$_9$O$_6$]** (δ = 0.97(2) mm/s, ΔE_Q = 1.12(2) mm/s). These data taken together support an all ferrous assignment.

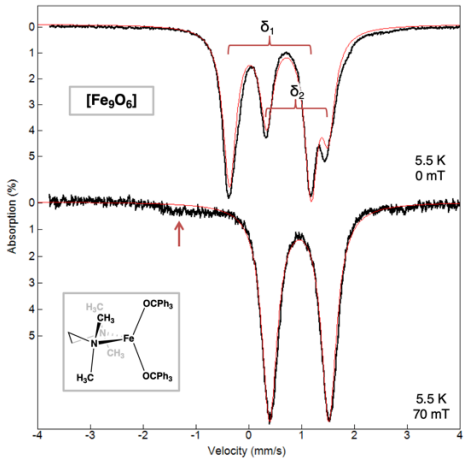

Figure 4. 5.5 K-Mössbauer spectra of crystalline **[Fe$_9$O$_6$]**•heptane (top, 0 T) and (tmeda)Fe($OCPh_3$)$_2$ (bottom, 70 mT). Data are shown in black hash-marks; the red lines are spectral fits with the parameters discussed in the text. Linewidths (FWHM) are 0.33 mm/s for **[Fe$_9$O$_6$]** and 0.30 mm/s for (tmeda)Fe($OCPh_3$)$_2$. The maroon arrow in the bottom panel indicates a broad, unidentified impurity accounting for less than 2 % of the total spectral area.

The low coordination geometry and weak ligand fields in **[Fe$_9$O$_6$]** should lead to high-spin configurations for all ferrous ions, but the magnetic behavior of the cluster is not as easy to predict. Coupling between magnetic ions mediated by a diamagnetic bridge would generally favor antiferromagnetic coupling,[28,29] but the threefold symmetry and odd number of iron atoms leads to a degree of magnetic frustration and an inability to completely quench the net magnetic moment.[30] Accordingly, Evans method measurements (Figure 5, left) reveal that solutions of **[Fe$_9$O$_6$]** at 298 K exhibit an effective magnetic moment that is

lower than that expected for nine non-interacting high-spin Fe(II) centers (7.9 instead of 14.7), but considerably *higher* than expected for nine antiferromagnetically-coupled high-spin Fe(II) centers (net S = 2, expected μ_{eff} value ≅ 4.9). This implies considerable (but not maximal) antiferromagnetic coupling between the ferrous centers.

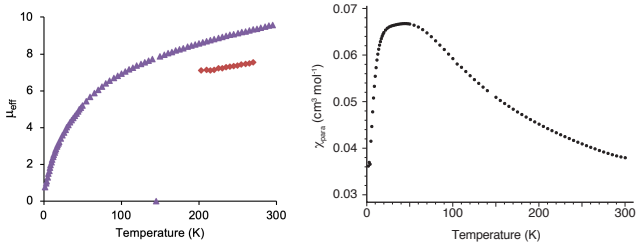

Figure 5. Left: Effective magnetic moment of **[Fe_9O_6]** in the solid state (SQUID, 1 T, purple) and in THF-d_8 solution (400 MHz ^{1}H NMR, maroon). Right: variable-temperature magnetometry of crystalline **[Fe_9O_6]**•heptane (SQUID, DETAILS, left) at 0.5 T and 1T.

The solution-phase magnetic moment is weakly temperature dependent over the range from 200 K to 298 K, suggesting the complex has an S = 2 ground state with low-lying excited states that are thermally-accessible. Electronic structure calculations of a truncated model of the cluster ($Fe_9O_6(H)_6(NH_3)_6$) using the broken-symmetry formalism[31,32] are consistent with strong antiferromagnetic coupling leading to an S = 2 ground state (5 α Fe(II) + 4 β Fe(II)), with an energetically-accessible S = 6 excited state (6 α Fe(II) + 3 β Fe(II), +6.8 kcal/mol, expected μ_{eff} value = 13.0). The two electronic configurations differ in the relative spin orientation of one of the axial Fe atoms, wherein the first excited state has all the axial Fe environments antiferromagnetically coupled to the equatorial environments (Figure S4).

Magnetic susceptibility measurements performed on *solid* samples of **[Fe_9O_6]**•heptane reveal a higher effective magnetic moment value than found in solution (9.5 vs. 7.9 at 298 K). Upon decreasing the temperature, the effective magnetic moment value decreases monotonically, eventually reaching 0.8 at 2 K. This very low value implies that complexes are coupling with each other to lead to an overall singlet ground state. The temperature dependence of the molar magnetic susceptibility (χ_{para}) reveals Curie-Weiss behavior from 300 K to ~ 60 K (θ_P = –186 K at 1.0 T), whereupon the susceptibility levels out and then begins to decline below 20 K (Figure 5, right). The leveling-out behavior appears to be due to *two* discrete magnetic ordering events, occurring at 60 K and 20 K, which is unusual for molecular materials exhibiting simple antiferromagnetic coupling. It is conceivable that the events are due to the magnetic susceptibility anisotropy of crystalline **[Fe_9O_6]**, resulting in different energies for antiferromagnetic ordering of **[Fe_9O_6]** in the axes that are perpendicular and parallel to the magnetic field. Crystals of **[Fe_9O_6]** are axially symmetric (i.e. x = y ≠ z) (Figure 2) and interactions between clusters in the solid state may lead to complex magnetic behavior in polycrystalline samples, including multiple ordering events to relieve frustration. Using the higher ordering temperature (T_o) of 60 K, the degree of frustration (as $f = -\theta_P/T_o$)[33] of crystalline **[Fe_9O_6]**•heptane is calculated to be 3.10 at 1.0 T, indicating that this system is moderately frustrated. More in-depth magnetic studies of this system are currently underway.

Although the mechanism of formation of **[Fe$_9$O$_6$]** is difficult to elucidate, decades of research into the autoxidation of organometallic compounds, generally studied within the context of catalytic substrate oxidation, reveals that such reactions almost always favor free-radical chains.[34] Even noble metal organometallic systems, which usually terminate in alkoxide products from *formal* O-atom insertion into M-C bonds,[35–37] have been shown to proceed *via* radical steps initiated by binding of O_2 and formation of O-centered radicals. For iron-specific systems, Power has shown that Fe-aryl complexes exhibit formal O=O scission and O-atom insertion into M-C_{aryl} bonds.[38,39] In an extensive DFT study on the related O_2 reaction with the two-coordinate compound $FeMe_2$,[40] Cundari reported that the O-atom insertion is calculated to proceed *via* initial formation of open-shell Fe^{III}-(O_2^-) species and eventual generation of dioxo intermediates (as seen in Cr oxidation chemistry reported by Theopold)[41] prior to O-atom insertion into the Fe-C bonds. Additionally, Chirik has shown that ferrous dialkyls are susceptible to Fe-C homolysis upon addition of π-acidic redox-active ligands,[42] suggesting that coordination of O_2 could lead to the generation of free alkyl radicals. The reactions between O_2 and free alkyl radicals are essentially diffusion-controlled,[43,44] thus the observed neopentanol and pivalaldehyde could be the result of rapid oxidation of neopentyl radicals produced upon coordination of O_2 to (tmeda)Fe($CH_2{}^tBu)_2$. Oxidations under high concentrations of (tmeda)Fe($CH_2{}^tBu)_2$ seem essential, as the yield of **[Fe$_9$O$_6$]** was maximized *only* when the amount of residual (tmeda)Fe($CH_2{}^tBu)_2$ remained high (10 – 15%) – that is, reactions run to *complete* consumption of the dialkyl precursor actually resulted in *lower* yields of **[Fe$_9$O$_6$]** (< 5%). It is also notable that oxidation of (tmeda)Fe($CH_2{}^tBu)_2$ produces isolable amounts **[Fe$_9$O$_6$]** in either toluene or THF, but performing the same oxidation in pentane yields no isolable organometallic products. Given the weak C–H bonds in both toluene and THF, it seems plausible that these solvents are intercepting transient LFe^{III}-(O_2^-) species *via* formal H-atom transfer and minimizing the rate of aggregation and precipitation bulk iron oxide (Scheme 1).

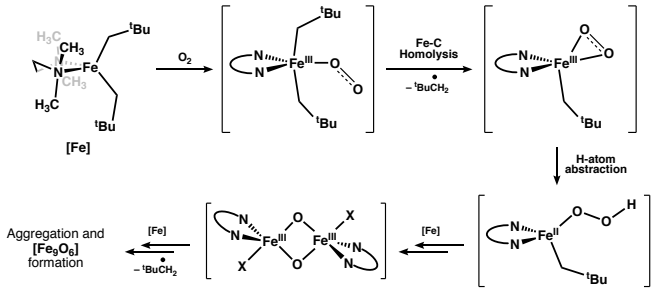

Scheme 1. One of the many possible oxidation cascade reactions leading to Fe-O bond formation during self-assembly of **[Fe$_9$O$_6$]**, where X indicates either neopentyl or alkoxide anionic ligands.

Among the most notable aspects of this reaction is that since oxidation of Fe(II) precursors yields only Fe(II) oxide materials, it is the iron-carbon bonds that are supplying the reducing equivalents. Low-coordinate organometallic complexes of first-row transition elements have considerable ionic character, and it seems possible that isolation of organometallic oxide clusters under substoichiometric oxidation conditions may be generalizable. Given the relatively low yield, the production of **[Fe$_9$O$_6$]** may be more a result of adventitious crystallization from a mixture of related clusters then the selective formation of just that

core, but it is notable that the core bears the same Fe_nO_m stoichiometry as one of the 'magic-sized' clusters first observed by Sun *et al.* in gas phase experiments.[15,16] Such patterns are observed in noble metal and semiconductor cluster chemistry,[4,12] wherein part of the ability to isolate monodisperse clusters relies on magic numbers of elements that have a particular stability as monomers aggregate. Despite the presence of ligands and different oxidation state, the topology of the metal oxide core in **[Fe_9O_6]** is the same as predicted for the unligated cluster.

The self-assembly of a complex, reduced, low-coordinate organometallic cluster provides unique opportunities in synthetic chemistry. Gentle heating (65 ºC) of **[Fe_9O_6]** over the course of several hours in benzene, for example, results in the formation of dark precipitate and the formation of neopentane, suggesting **[Fe_9O_6]** is capable of C–H activation in a similar manner as related low-coordinate iron complexes.[45] Simply exposing toluene solutions of **[Fe_9O_6]** to additional oxygen leads to the formation of polycrystalline nanoparticles of magnetite, as shown by electron diffraction studies. The intrinsic reactivity of **[Fe_9O_6]** and related clusters are currently under study for potential catalytic and nanomaterials applications. Of particular interest is the generality of such oxidative self-assembly; although a great deal of work has revealed the many ways iron organometallics can react under *reducing* conditions to yield catalytically relevant species,[46–49] the possibility of trace oxygen contamination and subsequent aggregation adds a new dimension of complexity.

Acknowledgements

Generous support from the University of Wyoming Research Office, the UW Department of Chemistry, and the UW School of Energy Resources is gratefully acknowledged. We also thank the UW Center for Photoconversion and Catalysis and NSF EPSCoR for undergraduate research fellowships (JAK). We would also like to thank Mr. Steve Adams and Mrs. Jane Adams of Cheyenne, WY for the generous donation of glassware. The authors gratefully acknowledge financial support from the National Science Foundation (CHE 0619920) for the purchase of the Bruker Apex II Diffractometer and National Institute of General Medical Sciences of the National Institutes of Health (from the Institutional Development Award, Grant # 2P20GM103432) for the purchase of the Oxford Cobra Cryo system. DFT calculations were performed on an allocation at the Advanced Research Computing Center at the University of Wyoming ("Teton", https://doi.org/10.15786/M2FY47). We gratefully acknowledge Prof. Caleb Hill's (UW) and Dr. Keith Carron's (Metrohm Raman, Laramie WY) multiple attempts at measuring Raman spectra of **[Fe_9O_6]**. We are also indebted to Prof. Dean Roddick (UW) and Prof. Richard Finke (CSU) for helpful discussions. Dr. Popescu thanks the National Science Foundation Grant NSF-RUI 1445959, the University of St. Thomas (MN) and The College of Arts and Sciences for their generous support. BNL and MPS thank the NSF (CHE-1363274 and CHE-1800554) for support of solid state magnetic studies.

References

(1) Castleman, A. W.; Jena, P. *Proc. Natl. Acad. Sci.* **2006**, *103* (28), 10554–10559.
(2) Wan, X.-K.; Yuan, S.-F.; Tang, Q.; Jiang, D.; Wang, Q.-M. *Angew. Chemie Int. Ed.* **2015**, *54* (20), 5977–5980.
(3) Jin, R. *Nanotechnol. Rev.* **2012**, *1* (1), 31–56.
(4) Cossairt, B. M. *Chem. Mater.* **2016**, *28* (20), 7181–7189.
(5) Friedfeld, M. R.; Stein, J. L.; Cossairt, B. M. *Inorg. Chem.* **2017**, *56* (15), 8689–8697.
(6) Beecher, A. N.; Yang, X.; Palmer, J. H.; Lagrassa, A. L.; Juhas, P.; Billinge, S. J. L.; Owen, J. S. *J. Am. Chem. Soc.* **2014**, *136* (30), 10645–10653.
(7) Owen, J.; Brus, L. *J. Am. Chem. Soc.* **2017**, *139* (32), 10939–10943.
(8) Goh, C.; Segal, B. M.; Huang, J.; Long, J. R.; Holm, R. H. *J. Am. Chem. Soc.* **1996**, *118* (47), 11844–11853.
(9) Roy, X.; Lee, C.-H.; Crowther, A. C.; Schenck, C. L.; Besara, T.; Lalancette, R. A.; Siegrist, T.; Stephens, P. W.; Brus, L. E.; Kim, P.; et al. *Science (80-.).* **2013**, *341* (6142), 157–160.
(10) Hernández Sánchez, R.; Betley, T. A. *J. Am. Chem. Soc.* **2015**, *137* (43), 13949–13956.
(11) Hernández Sánchez, R.; Bartholomew, A. K.; Powers, T. M.; Ménard, G.; Betley, T. A. *J. Am. Chem. Soc.* **2016**, *138* (7), 2235–2243.
(12) Gary, D. C.; Flowers, S. E.; Kaminsky, W.; Petrone, A.; Li, X.; Cossairt, B. M. *J. Am. Chem. Soc.* **2016**, *138* (5), 1510–1513.
(13) Bosch, M.; Yuan, S.; Rutledge, W.; Zhou, H.-C. *Acc. Chem. Res.* **2017**, *50* (4), 857–865.
(14) Fernando, A.; Weerawardene, K. L. D. M.; Karimova, N. V.; Aikens, C. M. *Chem. Rev.* **2015**, *115* (12), 6112–6216.
(15) Wang, Q.; Sun, Q.; Sakurai, M.; Yu, J. Z.; Gu, B. L.; Sumiyama, K.; Kawazoe, Y. *Phys. Rev. B* **1999**, *59* (19), 12672–12677.
(16) Sun, Q.; Sakurai, M.; Wang, Q.; Yu, J. Z.; Wang, G. H.; Sumiyama, K.; Kawazoe, Y. *Phys. Rev. B* **2000**, *62* (12), 8500–8507.
(17) Yin, S.; Xue, W.; Ding, X.-L.; Wang, W.-G.; He, S.-G.; Ge, M.-F. *Int. J. Mass Spectrom.* **2009**, *281* (1–2), 72–78.
(18) Bottomley, F.; Grein, F. *Inorg. Chem.* **1982**, *21* (12), 4170–4178.
(19) de Ruiter, G.; Thompson, N. B.; Lionetti, D.; Agapie, T. *J. Am. Chem. Soc.* **2015**, *137* (44), 14094–14106.
(20) Gorun, S. M.; Lippard, S. J. *Nature* **1986**, *319* (6055), 666–668.
(21) Barra, A. L.; Bencini, F.; Caneschi, A.; Gatteschi, D.; Paulsen, C.; Sangregorio, C.; Sessoli, R.; Sorace, L. *Chemphyschem* **2001**, *2* (8–9), 523+.
(22) Baca, S. G.; Speldrich, M.; Van Leusen, J.; Ellern, A.; Kögerler, P. *Dalt. Trans.* **2015**, *44* (17), 7777–7780.
(23) Kitos, A. A.; Papatriantafyllopoulou, C.; Tasiopoulos, A. J.; Perlepes, S. P.; Escuer, A.; Nastopoulos, V. *Dalt. Trans.* **2017**, 3240–3251.
(24) Yang, L.; Powell, D. R.; Houser, R. P. *Dalt. Trans.* **2007**, No. 9, 955–964.
(25) Noodleman, L.; Peng, C. Y.; Case, D. A.; Mouesca, J.-M. *Coord. Chem. Rev.* **1995**, *144* (C), 199–244.
(26) Beinert, H.; Holm, R. H.; Münck, E. *Science (80-.).* **1997**, *277* (5326), 653–659.
(27) Andres, H.; Bominaar, E. L.; Smith, J. M.; Eckert, N. A.; Holland, P. L.; Münck, E. *J. Am. Chem. Soc.* **2002**, *124* (12), 3012–3025.
(28) Kanamori, J. *J. Phys. Chem. Solids* **1959**, *10* (2–3), 87–98.
(29) Goodenough, J. B. *Chem. Mater.* **2014**, *26* (1), 820–829.
(30) *Introduction to Frustrated Magnetism*; Lacroix, C., Mendels, P., Mila, F., Eds.; Springer Series in Solid-State Sciences; Springer Berlin Heidelberg: Berlin, Heidelberg, 2011; Vol. 164.
(31) Noodleman, L. *J. Chem. Phys.* **1981**, *74* (10), 5737–5743.
(32) Ruiz, E. In *Comprehensive Inorganic Chemistry II*; Elsevier, 2013; Vol. 9, pp 501–549.
(33) Ramirez, A. P. *Annu. Rev. Mater. Sci.* **1994**, *24* (1), 453–480.
(34) Boisvert, L.; Goldberg, K. I. *Acc. Chem. Res.* **2012**, *45* (6), 899–910.
(35) Rostovtsev, V. V; Labinger, J. A.; Bercaw, J. E.; Lasseter, T. L.; Goldberg, K. I. *Organometallics* **1998**, *17* (21), 4530–4531.

(36) Prantner, J. D.; Kaminsky, W.; Goldberg, K. I. *Organometallics* **2014**, *33* (13), 3227–3230.
(37) Popp, B. V.; Stahl, S. S. *J. Am. Chem. Soc.* **2007**, *129* (14), 4410–4422.
(38) Ni, C.; Power, P. P. *Chem. Commun.* **2009**, No. 37, 5543.
(39) Zhao, P.; Lei, H.; Ni, C.; Guo, J.-D.; Kamali, S.; Fettinger, J. C.; Grandjean, F.; Long, G. J.; Nagase, S.; Power, P. P. *Inorg. Chem.* **2015**, *54* (18), 8914–8922.
(40) Prince, B. M.; Cundari, T. R.; Tymczak, C. J. *J. Phys. Chem. A* **2014**, *118* (46), 11056–11061.
(41) Dai, F.; Yap, G. P. A.; Theopold, K. H. *J. Am. Chem. Soc.* **2013**, *135* (45), 16774–16776.
(42) Fernández, I.; Trovitch, R. J.; Lobkovsky, E.; Chirik, P. J. *Organometallics* **2008**, *27* (1), 109–118.
(43) Wu, D.; Bayes, K. D. *Int. J. Chem. Kinet.* **1986**, *18* (5), 547–554.
(44) Sun, H.; Bozzelli, J. W. *J. Phys. Chem. A* **2004**, *108* (10), 1694–1711.
(45) MacLeod, K. C.; Lewis, R. A.; DeRosha, D. E.; Mercado, B. Q.; Holland, P. L. *Angew. Chemie Int. Ed.* **2017**, *56* (4), 1069–1072.
(46) Al-Afyouni, M. H.; Fillman, K. L.; Brennessel, W. W.; Neidig, M. L. *J. Am. Chem. Soc.* **2014**, *136* (44), 15457–15460.
(47) Muñoz III, S. B.; Daifuku, S. L.; Brennessel, W. W.; Neidig, M. L. *J. Am. Chem. Soc.* **2016**, *138* (24), 7492–7495.
(48) Kneebone, J. L.; Brennessel, W. W.; Neidig, M. L. *J. Am. Chem. Soc.* **2017**, *139* (20), 6988–7003.
(49) Muñoz, S. B.; Daifuku, S. L.; Sears, J. D.; Baker, T. M.; Carpenter, S. H.; Brennessel, W. W.; Neidig, M. L. *Angew. Chemie* **2018**, *130* (22), 6606–6610.